# Ni(111) surface state observed with scanning tunneling microscopy

K.-F. Braun*
*Department of Physics, Ohio University, Athens, 45701 Ohio, USA*
*Institut für Experimentalphysik, Freie Universität Berlin, Arnimallee 14, D-14195 Berlin, Germany*

K.-H. Rieder
*Institut für Experimentalphysik, Freie Universität Berlin, Arnimallee 14, D-14195 Berlin, Germany*
(Received 2 August 2007; revised manuscript received 29 February 2008; published 20 June 2008)

A high-resolution spectroscopy study of the electronic structure of the Ni(111) surface by scanning tunneling microscopy is presented. From the standing-wave pattern the electron dispersion of the surface state is determined using Fourier transform methods and compared with previous photoemission data. The dispersion parameters are found to change over a length scale of 30 nm whereas two dispersions with different binding energies but the same effective mass are found. The shifted dispersions could be resolved simultaneously at certain regions of the open terrace showing a splitting of the surface state by $\Delta E = 60 \pm 15$ meV.

DOI: 10.1103/PhysRevB.77.245429 PACS number(s): 68.47.De, 68.37.Ef, 73.20.−r

Scanning tunneling spectroscopy (STS) has been developed into an alternative approach to the more traditional photoelectron spectroscopic techniques for characterizing the electronic structure at surfaces. As main advantages, STS employs a highly local probe (the scanning tunneling microscopy (STM) tip) and allows detecting both occupied and empty states around the Fermi level by simply inverting the sign of the applied bias. However, it also suffers severe shortcomings such as the lack of $k$-space resolution or the fact that the measured signal is a convolution of the surface and tip electronic structure. A leap forward was achieved by performing STS experiments on standing-wave (SW) patterns associated to surface states that are typically formed at steps or around impurities.[1] In this way, $k$ resolution can be achieved after relating the bias dependence of the SW frequency to the surface band dispersion energy. STS on magnetic surfaces has also attracted much research interest during the last decade.[2–4] SW patterns of spin-polarized states of $d$ symmetry have been identified for Co islands on Cu(111) (Ref. 3) or Fe films on W(110).[4] However, the capability of STS to resolve spin-polarized $sp$ bands, typically displaying a much smaller exchange split ($\approx$100 meV), has not yet been demonstrated.

On the theoretical side, density functional theory (DFT) (Ref. 5) based calculations represent nowadays the most popular framework for predicting the band structure of periodic systems. However, quantitative and, particularly in magnetic systems, qualitative disagreements between DFT results and experimental spectra have been routinely reported and mainly assigned to the local character of the exchange and correlation energy inherent in this theory. Corrections to this approach, such as the so-called LDA+$U$,[6] self-interaction corrections,[7] or charge-transfer models,[8] have circumvented this failure, but still a unified and robust scheme to accurately describe electron-electron and electron-hole correlations is still lacking.

A prototypical example of all the above problems is the unreconstructed Ni(111) surface—a 3$d$ metal ferromagnetic surface. Despite long withstanding experimental and theoretical effort, the precise electronic structure of this system remains unresolved. Early spin-resolved inverse photoemission spectroscopy (IPES) experiments reported the existence of a spin-polarized surface state of $p$ character close to the $\bar{\Gamma}$ point with an upward dispersion and an exchange splitting close to 100 meV.[9] The majority-spin component was found below the Fermi level while it was not clear whether the minority band was partially occupied or fully empty. A second surface state, fully occupied and dispersing downward, could also be resolved.[9] Spin averaged photoemission spectroscopy (PES) experiments later confirmed the existence of both surface states: a partially occupied surface band with an upward dispersion (S1 band) as well as the downward dispersing band (S band).[10] STS experiments have also been performed for dislocation structures on Ni(111),[11] where the Shockley-type S1 state could be identified from SW patterns. Unfortunately, the STS spectra did not resolve any magnetic splitting, even though it has been suggested theoretically that spin-polarized SW patterns should be attainable on this surface.[12] Although a wide variation of values for the Ni(111) surface has been obtained theoretically,[12–15] none of them have accurately reproduced the S1 and S surface-state bands.

In this paper we report an investigation with the STM on the Ni(111) surface. STS data were recorded and analyzed following two different approaches: (a) applying Fourier transform methods to SW patterns generated around single impurities and (b) recording line scans at SW wave fronts appearing at the step edges. As our central result, we have determined with high accuracy the surface-state binding energy and effective mass following both approaches. The dispersion parameters were found to depend on the location and two surface-state bands shifted against each other were found.

The Ni sample was cleaned with sputter cycles using $Ne^+$ ions followed by annealing cycles with temperatures up to 1300 K. Prior to the last cycle 10 L of oxygen were dosed in order to remove remaining carbon and hydrogen atoms. Remaining concentrations of adsorbates showed to be sensitive to the residual gas pressure and the annealing temperature. The sample was subsequently cooled with liquid helium before transferring it into the microscope.[16] All measurements

 

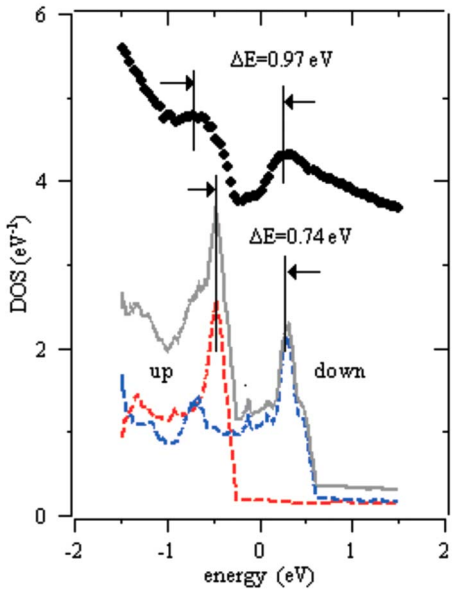


FIG. 1. (Color online) The upper graph shows a $dI/dV$ point spectrum from a defect free Ni(111) terrace with two broad maxima above and below the Fermi energy. The lower graphs correspond to the PBE calculated spin-resolved DOS.

were done at 5 K and Au atoms were evaporated *in situ* at the same temperature.

We first address single point spectra taken in defect-free areas on the open terrace. The STS data presented in Fig. 1 show two pronounced maxima close to the Fermi energy and separated by an energy gap of 0.97 eV. In the lower part of the figure the calculated density of states (DOS) projected onto Ni bulk atoms is displayed. DFT under the generalized gradient approximation Perdew-Burke-Ernzerhof[17] (PBE) employing plane waves was used and resulted in a value of 0.74 eV for the spin split energy between two bulk $d$ bands.[18] A surface slab calculation with 24 layers and projection on the surface atoms showed practically the same results with minor shifts of the energies. Although the calculated curve displays the bare DOS it serves here as an approximation for the local density of states (LDOS) at the tips position above the surface and is therefore compared directly to the experimental curve. Given the close correlation between the experimental and both theoretical curves, we assign the energy gap to the exchange-split energy of the Ni $d$ bands. Hence, the maximum above the Fermi energy stems solely from the minority-spin component, while the one below contains contributions from both spins. From the comparison it is, however, not possible to establish whether the maxima correspond to the surface or bulk $d$ states.

Next, we concentrate on the SW patterns created by remaining adsorbed impurities as well as by purposely adsorbing gold atoms on the surface. This set of experiments was carried out by choosing large terraces and recording $dI/dV$ area maps in a constant-current mode. The surface electrons were investigated over an energy interval ranging from −200 up to +400 meV with an initial impurity concentration of $10^{-4}$ and increased up to $10^{-3}$ after adding single Au atoms. The spectroscopic maps shown in Figs. 2(a) and 2(d) reveal Friedel oscillations resolved below and above the Fermi energy. In both figures bright (high electron density) and darker (low-density) areas can be distinguished. Close to step edges [Fig. 2(a)], the bright areas are always located on the upper terrace, while the depleted areas are found in the lower one. For SWs on open terraces, they are randomly distributed [see Fig. 2(d)]. The spatial extent of such areas is around 30 nm. The corresponding power spectra, displayed in Figs. 2(b) and 2(e), exhibit circular contours with radial distributions containing well-defined maxima [Figs. 2(c) and 2(f)], thus allowing to determine the crystal momentum values with high accuracy. Remarkably, we note the two isotropic circular contours clearly resolved in Figs. 2(e) and 2(f). Such double ring structure is visible only in the bright areas of the image and not in the depleted (darker) areas.

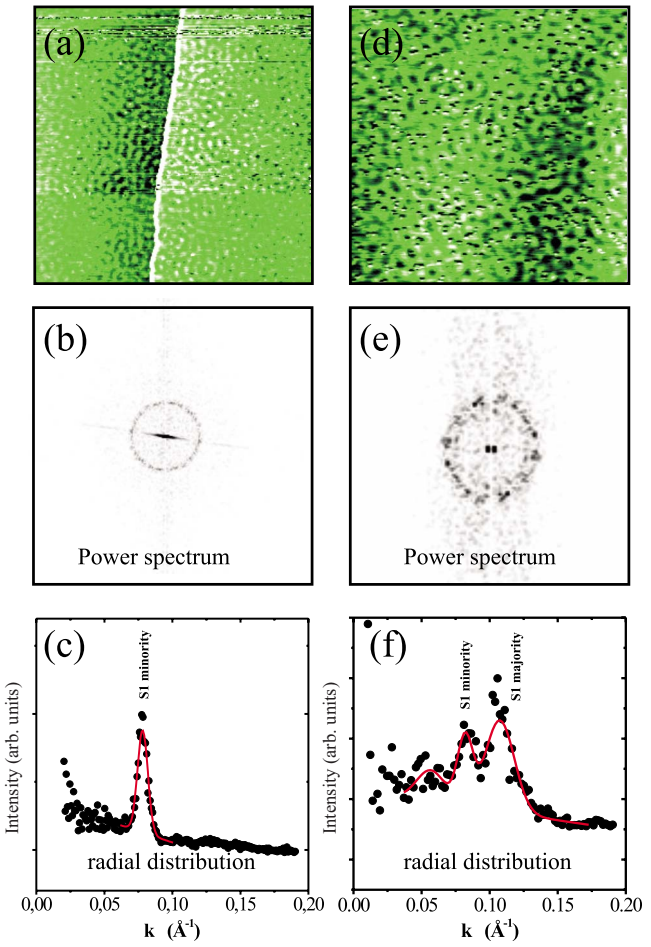


FIG. 2. (Color online) The spectroscopic maps show energy resolved Friedel oscillations from (a) impurities ($U=-26$ meV, $126\times126$ nm$^2$) and (d) Au atoms ($U=+56$ meV, $63\times63$ nm$^2$). [(b) and (e)] The power spectra show circular contours and allow to determine precisely the corresponding wave vector from the radial distribution in (c) and (f).

Finally, we have also measured SWs created at the step edges. Here, the translational invariance of the SW pattern allowed us to use line scans taken perpendicular to the step edge, such as those displayed in Fig. 3(a). Each plot in the figure is thereby the sum of 128 line scans recorded at the same energy. Care was taken to choose defect-free areas and to use straight close-packed steps. The momentum values

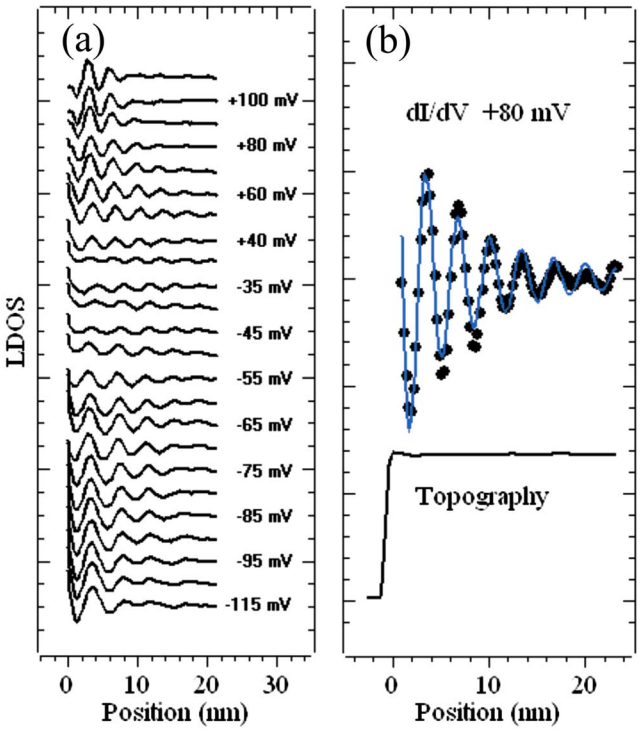


FIG. 3. (Color online) (a) Spectroscopic data consisting each of the sum of 128 line scans perpendicular to a step edge. The energies range from −115 to +110 meV in 5 and 10 meV steps. (b) The $dI/dV$ signal is recorded in constant-current mode on top of an unperturbed topography. From the least-squares fit to a damped oscillating wave function the wave vector is determined (Refs. 19 and 20).

were obtained by least-squares fitting of the decaying wave to an exponentially damped zeroth-order Bessel function.[19,20] The use of one-dimensional line scans avoids momentum contributions from scattering parallel to the step edge. Although the momentum space is therefore confined to values in one direction, this approach provided a higher accuracy for the SW wave vector than the use of two-dimensional Fourier transformations which were used for the evaluation for the data on the terrace.[21]

The combined results of both sets of experiments are put together in Fig. 4. The electron energies versus their momentum values show either one or two upward dispersing branches. The values follow closely a quadratic profile for negative voltages while they become more linear at higher positive voltage. Some data points are scattered beyond statistical error estimates, away from the progression of the two dispersions. We attribute these deviations to the appearance of maxima in the radial distributions which do not stem from surface states. As example we point out that in Fig. 2(f) three maxima occur although only two of them can be assigned to the surface electrons with a circular contour in Fourier space (cf. Fig. 2(e), above). For completeness all maxima are included. From the spectra below the Fermi energy, binding energies of $E_B=-165\pm4$ meV and $E_B=-225\pm11$ meV and effective electron masses of $m^*=(0.169\pm0.005)m_e$ and $m^*=(0.17\pm0.01)m_e$ are determined for each of the two resolved bands. Thereby a quadratic form of the electron dispersion was assumed.

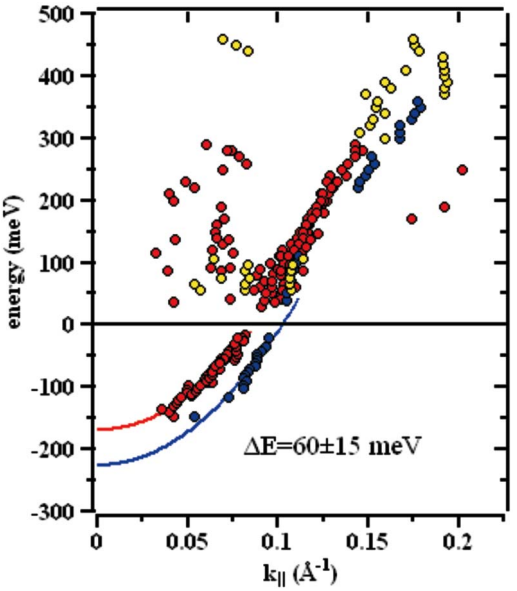


FIG. 4. (Color online) The combined results show two electron dispersion branches offset by an energy of $\Delta E=60\pm15$ meV. The blue circles represent data at the step edge, the red circles stem from the terrace, and the yellow circles are data on the open terrace where both dispersions are observed simultaneously. The data below the Fermi energy have a parabolic shape with binding energies $E_B=-165$ meV and $E_B=-225$ meV. In both cases the effective-mass amounts to $m^*=0.17m_e$.

Comparing the obtained values of the surface dispersion with other experiments one gets fairly good agreement. First the dispersion parameters of the surface electrons are reproduced if compared to the spin-averaged PES results in Ref. 10. There a value of $m^*=(0.13\pm0.05)m_e$ is obtained with a band minimum of $E_B=-110\pm20$ meV. For comparison with our data we extrapolate this room-temperature value down to 5 K and estimate $E_B=-160\pm20$ meV.[22] Furthermore from the spin-averaged data the width of the photoemission maxima was evaluated. A curve form analysis yielded thereby an estimate of the spin splitting of $\Delta E_{\mathrm{PES}}=20-70$ meV which separates the dispersion branches of the minority-spin component from the majority-spin component.[10,23] Moreover, in Ref. 9 spin-resolved photoemission spectroscopy has determined a value of $\Delta E_{\mathrm{PES}}=106\pm22$ meV for the magnetic exchange splitting above the Fermi level at an energy of +0.74 eV. This is in good agreement with values of $\Delta E_{\mathrm{STM}}(\Gamma)=60\pm15$ meV at the $\Gamma$ point obtained here. Consequently we interpret our observed splitting into two dispersion branches as a magnetic exchange splitting of the surface state. Finally we want to compare our results with those obtained with scanning tunneling spectroscopy in Ref. 11. There spin-averaged STS data of confined electrons in dislocation structures have yielded different values of $E_B=-70\pm20$ meV and $m^*=(0.24\pm0.04)m_e$. The confinement of electrons in a nanostructure is well known to result solely in a quantization and to leave the dispersion otherwise unperturbed.[24] From our observations on the other hand we expect the appearance of one spin component only since the nanostructure encloses a bright area. We conclude that the use of a hard wall model,

the use of a purely parabolic dispersion, and an experimental broadening of 100 meV are the reasons for the higher binding energy.

Comparing the obtained values of the surface dispersion with theoretical results one gets less good agreement. The full-potential linearized augmented plane-wave (FLAPW) method within the local spin-density approximation was used to calculate the electronic structure of the Ni(111) surface.[25,26] The main experimental features observed in previous PES experiments can be readily identified in these theoretical bands. More precisely, the spin-exchange splitted band S1 is reproduced with a curvature described by an effective mass close to $m^*=(0.13\pm0.04)m_e$.[27] The calculated majority band S1 is partially occupied, while the minority component is empty. The binding energies amount to $E_B=-5$ meV for the majority[25] and $E_B=150\pm10$ meV for the minority-spin component.[27] Binding energies as well as the magnetic exchange split of $\Delta E_{\mathrm{DFT}}(\Gamma)=155\pm10$ meV have values above those experimentally determined. Two downward dispersing branches can be ascribed to the S band. Apart from these two well reported states, an intense and almost flat band for the minority-spin component also appears at +150 meV. Presumably due to its lack of dispersion it is absent in the $dI/dV$ area maps. Reference 15 employs a self-consistent tight-binding linear muffin-tin orbital (TB-LMTO) method and reports an even larger spin splitting of $\Delta E_{\mathrm{TB\text{-}LMTO}}(\Gamma)=430\pm10$ meV. Again one spin component of the S1 state is occupied while the other is not. Although the general features of the experimental results are reproduced by theory, a quantitative disagreement has to be reported. In particular the values for the spin splitting range above those obtained experimentally. This has to be assigned mainly to an insufficient treatment of the exchange and correlation energy inherent in the used theories.[28] Finally, calculations were performed within DFT and the projector augmented wave (PAW) approach.[12] Both spin components of the surface state appear to be unoccupied but with $E_B=+55$ meV close to the Fermi energy. The spin splitting of the Shockley state is $k$ dependant and is reported to be $\Delta E_{\mathrm{PAW}}(\Gamma)=20$ meV at the $\Gamma$ point and reaches $\Delta E_{\mathrm{PAW}}=0.34$ eV at $k=0.29$ Å$^{-1}$. A partial agreement with the experimental results is found.

According to our interpretation we assign the red data points in Fig. 4 to the minority-spin component, the blue data points to the majority-spin component, and the yellow data points to both of them. We rule out a tip effect causing the splitting between the blue and the red data points because the spectroscopic data are recorded in area maps. Any influence of the electronic structure of the tip is independent of the tip spatial position and contributes therefore only a constant background. Furthermore the bluntness of the tip plays a minor role as well as long as the resolution is better than the wavelength of the standing waves; in conclusion we rule out tip effects in the spectroscopic area results.

Next we want to rule out contributions other than from the surface states to the data in Fig. 4. Bulk electronic states can, in principle, give rise to SW pattern at surfaces as well.[29] However we can exclude contributions from the edge of the projected bulk band gap here due to their different symmetry properties. In Ref. 30 the Fermi-surface map of the Ni(111) surface shows a threefold symmetry for the gap while the two concentric rings in Fig. 4(e) are isotropic. Therefore we are dealing here with surface electrons only.

We finally want to rule out a possible electric-field effect being reason for the observed splitting between blue and red data points of Fig. 4 caused by different tips. A field effect on the Ni(111) surface has been explicitly calculated by Ohwaki *et al.*[25] Rather strong electric fields can therefore cause a downward shift of the surface-state onset by 15 meV with fields of 1 V/nm. An even stronger Stark effect has been observed experimentally in a tunneling junction on Ag, Cu, and Au surfaces.[31,32] However such an effect has been obtained only upon lowering of the tunneling resistance from gigaohms to kilohms over 4 orders of magnitude. In contrast, in our experiments the tunneling resistance was kept constant and so was the distance to the surface. Switching to different tip geometries at the same distance is not expected to influence the electric field. The same tip preparation in all measurements on the other hand warrants a metallic apex and hence the same electric field.[33] We therefore rule out an electric-field effect.

The majority-spin component was systematically resolved at the step edge, while the minority-spin component was resolved on the terrace.[34] This corresponds to the blue and red circles of the lower and upper branches of the dispersion in Fig. 4. It is this systematic which lets us propose a spin dependent scattering mechanism for the step edge responsible for the attenuation and amplification of one or the other spin component, respectively. We finally point out that the upper step edge always has a higher density (bright area) than the lower step edge (dark area). This shows strongly asymmetric reflections for step-up and step-down scatterings. A spin dependent scattering is well known and investigated for the Kondo resonance for single atoms, while the magnetic scattering at a step edge is less well understood.[35–37] We hope to motivate with this work a more thorough theoretical investigation of the intensity changes in the surface electronic structure close to the step edges.

In conclusion, we have demonstrated the capability of the STS technique to study the spin-polarized Ni(111) surface states. Surface band dispersions and values for the magnetic exchange splitting are obtained via this technique, yielding good agreement with PES results previously obtained for the same system. We hope this work will motivate further STS studies on 3$d$-magnetic surfaces.

We thank A. Govorov for interesting discussions. K.-F. B. acknowledges the computation Grant No. DMRR060005N from the National Center for Supercomputing Applications (NCSA).

*braun@phy.ohiou.edu

[1] M. F. Crommie, C. P. Lutz, and D. M. Eigler, Science **262**, 218 (1993); E. J. Heller, M. F. Crommie, C. Lutz, and D. M. Eigler, Nature (London) **369**, 464 (1994).
[2] K.-F. Braun, S. Fölsch, G. Meyer, and K.-H. Rieder, Phys. Rev. Lett. **85**, 3500 (2000).
[3] L. Diekhöner, M. A. Schneider, A. N. Baranov, V. S. Stepanyuk, P. Bruno, and K. Kern, Phys. Rev. Lett. **90**, 236801 (2003).
[4] K. von Bergmann, M. Bode, A. Kubetzka, M. Heide, S. Blügel, and R. Wiesendanger, Phys. Rev. Lett. **92**, 046801 (2004).
[5] P. Hohenberg and W. Kohn, Phys. Rev. **136**, B864 (1964); W. Kohn and L. J. Sham, *ibid.* **140**, A1133 (1965).
[6] V. I. Anisimov, F. Aryasetiawan, and A. I. Lichtenstein, J. Phys.: Condens. Matter **9**, 767 (1997).
[7] A. Svane and O. Gunnarsson, Phys. Rev. Lett. **65**, 1148 (1990).
[8] J. Zaanen, C. Westra, and G. A. Sawatzky, Phys. Rev. B **33**, 8060 (1986).
[9] M. Donath, F. Passek, and V. Dose, Phys. Rev. Lett. **70**, 2802 (1993).
[10] J. Kutzner, R. Paucksch, C. Jabs, H. Zacharias, and J. Braun, Phys. Rev. B **56**, 16003 (1997).
[11] S. Pons, P. Mallet, L. Magaud, and J.-Y. Veuillen, Europhys. Lett. **61**, 375 (2003).
[12] L. Magaud, A. Pasturel, P. Mallet, S. Pons, and J.-Y. Veuillen, Europhys. Lett. **67**, 90 (2004).
[13] G. Borstel, G. Thörner, M. Donath, V. Dose, and A. Goldmann, Solid State Commun. **55**, 469 (1985).
[14] F. Mittendorfer, A. Eichler, and J. Hafner, Surf. Sci. **423**, 1 (1999).
[15] J. Braun and M. Donath, Europhys. Lett. **59**, 592 (2002).
[16] N. Pertaya, K.-F. Braun, and K.-H. Rieder, Rev. Sci. Instrum. **75**, 2608 (2004).
[17] J. P. Perdew, K. Burke, and M. Ernzerhof, Phys. Rev. Lett. **77**, 3865 (1996).
[18] ESPRESSO, S. Baroni, A. Dal Corso, S. de Gironcoli, P. Giannozzi, C. Cavazzoni, G. Ballabio, S. Scandolo, G. Chiarotti, P. Focher, A. Pasquarello, K. Laasonen, A. Trave, R. Car, N. Marzari, and A. Kokalj (http://www.pwscf.org).
[19] L. Bürgi, O. Jeandupeux, H. Brune, and K. Kern, Phys. Rev. Lett. **82**, 4516 (1999).
[20] K.-F. Braun and K.-H. Rieder, Phys. Rev. Lett. **88**, 096801 (2002).
[21] No indication for more than one wave vector was found and therefore a single wave vector was used only.
[22] R. Paniago, R. Matzdorf, G. Meister, and A. Goldmann, Surf. Sci. **336**, 113 (1995).
[23] R. Paucksch, Ph.D. thesis, Universität-Gesamthochschule Essen, 2000.
[24] K. Morgenstern, K.-F. Braun, and K.-H. Rieder, Phys. Rev. Lett. **89**, 226801 (2002).
[25] T. Ohwaki, D. Wortmann, H. Ishida, S. Blügel, and K. Terakura, Phys. Rev. B **73**, 235424 (2006).
[26] J. Lobo-Checa, T. Okuda, M. Hengsberger, L. Patthey, T. Greber, P. Blaha, and J. Osterwalder, Phys. Rev. B **77**, 075415 (2008).
[27] This estimate has been taken from the graph of the calculated results in Ref. 25.
[28] F. Manghi, V. Bellini, J. Osterwalder, T. J. Kreutz, P. Aebi, and C. Arcangeli, Phys. Rev. B **59**, R10409 (1999).
[29] J. I. Pascual, A. Dick, M. Hansmann, H.-P. Rust, J. Neugebauer, and K. Horn, Phys. Rev. Lett. **96**, 046801 (2006).
[30] M. Hoesch, T. Greber, V. N. Petrov, M. Muntwiler, M. Hengsberger, W. Auwarter, and J. Osterwalder, J. Electron Spectrosc. Relat. Phenom. **124**, 263 (2002).
[31] L. Limot, T. Maroutian, P. Johansson, and R. Berndt, Phys. Rev. Lett. **91**, 196801 (2003).
[32] J. Kröger, L. Limot, H. Jensen, R. Berndt, and P. Johansson, Phys. Rev. B **70**, 033401 (2004).
[33] D. H. Huang, F. Grey, and M. Aono, Appl. Surf. Sci. **130–132**, 909 (1998).
[34] A similar observation of the difference in between scattering from point scatterers and scattering at the step edge has been mentioned briefly in Ref. 36 without further explanation.
[35] O. Pietzsch, S. Okatov, A. Kubetzka, M. Bode, S. Heinze, A. Lichtenstein, and R. Wiesendanger, Phys. Rev. Lett. **96**, 237203 (2006).
[36] J. Wiebe, F. Meier, K. Hashimoto, G. Bihlmayer, S. Blugel, P. Ferriani, S. Heinze, and R. Wiesendanger, Phys. Rev. B **72**, 193406 (2005).
[37] T. Kawagoe, E. Tamura, Y. Suzuki, and K. Koike, Phys. Rev. B **65**, 024406 (2001).